JOURNAL OF CATALYSIS 150, 274–283 (1994)

Energy Distribution of Surface Acid Sites of Metal Oxides

Paolo Carniti,* Antonella Gervasini,* and Aline Auroux†

*Dipartimento di Chimica Fisica ed Elettrochimica, Università di Milano, Via Golgi 19, 20133 Milano, Italy; and †Institut de Recherches sur la Catalyse, CNRS, Associé a l'Université Claude Bernard Lyon I, 2 Avenue Albert Einstein, 69626 Villeurbanne Cedex, France

Received August 25, 1993; revised March 7, 1994

The acid site strength distributions of γ-Al_2O_3, BeO, Nb_2O_5, TiO_2, WO_3, and ZrO_2 surfaces were evaluated starting from volumetric and calorimetric experimental data of ammonia adsorption collected at 80 and 150°C. A mathematical model was employed to describe the behavior of the adsorbate–adsorbent system. The model took into account a discrete inhomogeneity of the surface. A fitting procedure applied to both the isotherms and the integral heat curves of ammonia adsorption, at the two above temperatures, permitted the determination of the thermodynamic parameters characteristic of the different types of site. The number, $n_{max,i}$, the adsorption equilibrium constant, b_i, as well as a new parameter termed the "half-coverage temperature at unit pressure," $T^{\circ}_{1/2,i}$, of each type of acid site were obtained. All the oxides showed a significant amount of acid sites with ammonia enthalpy of adsorption $\Delta_a H_i$ at -40 kJ/mol corresponding to hydrogen-bonded ammonia. Three types of more energetic sites, with $\Delta_a H_i$ ranging from -280 to -160 kJ/mol, were found for γ-Al_2O_3, Nb_2O_5, TiO_2, and ZrO_2. Sites with $\Delta_a H_i$ of -280 and -200 kJ/mol were found for BeO and WO_3. Mean molar adsorption entropies were also determined, and the values obtained are typical of immobile or localized adsorption.

INTRODUCTION

The acidic properties of metal oxide surfaces, among other properties such as, for example, electron-donating properties, are of great importance in the interpretation of the behavior of these materials when they are used as catalysts or employed in other fields of science and technology (1).

Many physical and chemical methods for testing the acidity and the acid strength distribution have been developed. Tanabe *et al.* (2) distinguished two main methods for characterizing the acidity of surfaces: the titration method using indicators and the gas-phase adsorption method. The gas-phase adsorption method, in which different basic probe molecules are used as adsorbates, e.g., pyridine, ammonia, and acetonitrile, chosen on the basis of their basicity and molecular size, appears to be the most promising due to its wide application. It can be applied even on colored samples and is independent of the kind of surface acid sites, Brønsted, and/or Lewis.

To determine the distribution of the strength of surface acid sites, temperature programmed desorption (TPD) of adsorbed base molecules and adsorption calorimetry of base molecules are often used. TPD provides an acid strength distribution as a function of temperature through the determination of kinetic parameters of desorption (3, 4). Adsorption calorimetry, which allows simultaneously the collection of both volumetric and calorimetric data, gives a more direct evaluation of the energy distribution of acid sites and permits the determination of thermodynamic parameters of adsorption (5–7).

Most studies of adsorption calorimetry carried out to evaluate the energy distribution of acid sites on heterogeneous surfaces have been performed at only one temperature (7). In such studies, the strength and the number of sites are often evaluated on the basis of the form of curves of the differential heat of adsorption vs the amount of base molecules adsorbed. The different types of site are often assumed to be filled successively starting from the strongest ones. This assumption can hold only if large differences among the adsorption constants are involved (7).

Performing adsorption calorimetry measurements at different temperatures, different distributions of sites can be observed (7–9). If no modification of the surface occurs in the temperature range considered, the different observed distributions can be due to either kinetic or thermodynamic effects.

Regarding the kinetic effects, at low temperature, the strongest sites may not be activated or, even if activated, may be occupied at an adsorption rate too low to achieve equilibrium during the experiment. Moreover, surface diffusion can play an important role in the equilibration of the adsorbate if enough time does not elapse before the collection of data.

When the temperature and the time employed in the measurements ensure that the adsorption equilibrium has been obtained on all sites, the differences among the ob-

0021-9517/94 $6.00

served distributions have to be ascribed to the influence of temperature on the thermodynamic parameters of adsorption, particularly on the adsorption constants.

Only accurate measurements carried out at different temperatures can give the "true" site distribution. Besides, the thermodynamic parameters of adsorption can be obtained as functions of temperature. The "true" distribution can be different from the observed one obtained by using the above-mentioned oversimplification, which considers that the sites are successively covered starting from the strongest ones. As pointed out by Cardona-Martinez and Dumesic (7), the temperatures employed should be sufficiently high that the adsorption process is activated on all types of site, but low enough that the adsorption equilibrium constants are favorable.

In this work, the energy distribution of acid sites for six metal oxides of catalytic relevance, as well as the values of the thermodynamic parameters of adsorption with their dependence on temperature, have been optimized through a fitting procedure of the volumetric–calorimetric data of ammonia adsorption measured at two different temperatures.

EXPERIMENTAL

Materials

Six metal oxides differing in their acidic characteristics were chosen among those studied in previous works (10–12), namely γ-Al_2O_3, BeO, Nb_2O_5, TiO_2 (anatase), WO_3, and ZrO_2. They were all commercial materials of guaranteed degree of purity (>99.9%). The BET surface areas measured after thermal treatment of 400°C were 124, 45, 59, 120, 38, and 63 m^2/g for γ-Al_2O_3, BeO, Nb_2O_5, TiO_2, WO_3, and ZrO_2, respectively. Further details regarding the studied oxides are reported in Ref. (10).

Ammonia from Air Liquide (purity >99.9%) was purified on Na wire.

Methods

Volumetric and calorimetric measurements of NH_3 adsorption were performed in a differential heat-flow microcalorimeter of the Tian-Calvet type (HT from Setaram) linked to a volumetric line, equipped with a differential pressure gauge (Datametrics) which permitted the introduction of dosed gas. Successive NH_3 introductions were repeated until a final equilibrium pressure of 1 Torr was achieved. Both the volumetric and the calorimetric data were stored and analyzed by microcomputer processing. The isotherms, the differential (q) and the integral (Q) heats of NH_3 adsorption were obtained. Experimental procedure details are reported in Ref. (10).

New volumetric and calorimetric data collected at 80°C are presented in this work. Data at 150°C, already reported (10), were also utilized for the present computations.

Computations

The computations were performed on an IBM PS2-50Z personal computer and on an IBM RISC/6000-320 work station.

MATHEMATICAL MODEL

The overall adsorption isotherms were interpreted as summations of single Langmuir isotherms, each of them relevant to the sites of a definite type (7, 9, 13–16)

$$n = \sum_i n_i = \sum_i \frac{n_{\max,i} \cdot b_i \cdot p}{1 + b_i \cdot p}, \qquad [1]$$

where n is the total number of adsorbed moles at pressure p, n_i, and $n_{\max,i}$ are the actual and the maximum number of moles adsorbed on sites of the ith type, respectively, and b_i is the adsorption constant of the sites of the ith type which depends on temperature. Such a dependence can be obtained through the integration of the van't Hoff differential equation, considering the adsorption enthalpy ($\Delta_a H_i$) to be either independent, Eq. [2a], or dependent on temperature, Eq. [2b], respectively

$$b_i = b_{o,i} \cdot \exp(-\Delta_a H_i / RT) \qquad [2a]$$

$$b_i = b_{o,i} \cdot \exp(-\Delta_a H_i / RT + (\Delta_a C_{p,i}/R) \cdot \ln T), \qquad [2b]$$

where $\Delta_a C_{p,i}$, the heat capacity of adsorption, has to be used if the temperature range considered is not narrow enough for $\Delta_a H_i$ to be considered constant.

Also the integral heat of adsorption was considered as a summation:

$$Q = -\sum_i n_i \cdot \Delta_a H_i. \qquad [3]$$

On the basis of the experimental values of n and Q obtained at the two investigated temperatures as a function of pressure and of coverage, respectively, the characteristic parameters of adsorption ($n_{\max,i}$, $\Delta_a H_i$, and either $b_{o,i}$ or other parameters related to it, for each ith type of site) were evaluated by means of a computation program, including the optimization subroutine OPTNOV (17), which minimized the following objective function

$$\Phi = \sum_j \sum_k \frac{(n_{jk,\text{calc}} - n_{jk,\text{expl}})^2}{n_{jk,\text{expl}}^2} + \sum_j \sum_k \frac{(Q_{jk,\text{calc}} - Q_{jk,\text{expl}})^2}{Q_{jk,\text{expl}}^2} \qquad [4]$$

where $n_{jk,\text{expl}}$ and $Q_{jk,\text{expl}}$ refer to the experimental values at a given temperature (index j) and pressure (index k), and $n_{jk,\text{calc}}$ and $Q_{jk,\text{calc}}$ refer to the corresponding values calculated by Eqs. [1–3].

Assuming a nondissociative chemisorption of the adsorbate with 1 : 1 stoichiometry, the parameter $n_{\max,i}$ of Eq. [1] corresponds with the total number of ith type sites. The sum of all the values of $n_{\max,i}$ is equal to the total chemical monolayer ($n_{\max}$):

$$n_{\max} = \sum_i n_{\max,i}.$$

Considering the monolayer coverage of the whole surface as the maximum limit value of $n_{\max}$, the single $n_{\max,i}$ can be considered as a fraction of this limit. The monolayer coverage of the whole surface can be calculated on the basis of the cross-sectional area of the adsorbate.

As a characteristic parameter to be optimized, $b_{o,i}$ could be chosen, but the validity of this parameter is difficult to evaluate because it does not have a simple physical meaning and the range of its reasonable numerical values is far from being clearly defined (18). A new parameter related to $b_{o,i}$ and defined below, the "half-coverage temperature at unit pressure" ($T^{\circ}_{1/2,i}$), was introduced and optimized instead of $b_{o,i}$.

The new parameter has a more simple physical meaning and a more reasonable range of values than $b_{o,i}$. It corresponds to the temperature at which the adsorption constant b_i becomes unity. By employing Eq. [2a] or [2b], one obtains:

$$b_i = b_{o,i} \cdot \exp(-\Delta_a H_i/R \cdot T^{\circ}_{1/2,i}) = 1 \qquad [5a]$$

or

$$b_i = b_{o,i} \cdot \exp(-\Delta_a H_i/R \cdot T^{\circ}_{1/2,i} + (\Delta_a C_{p,i}/R) \cdot \ln T^{\circ}_{1/2,i}) = 1. \qquad [5b]$$

In the case of a Langmuir isotherm, the condition $b \cdot p = 1$ corresponds to half coverage. Therefore, the sites of the ith type are half-covered at $T = T^{\circ}_{1/2}$ at unit pressure:

$$\frac{n_i}{n_{\max,i}} = \frac{b_i \cdot p}{1 + b_i \cdot p} = \frac{1}{2}.$$

The relation between $b_{o,i}$ and $T^{\circ}_{1/2,i}$ can be derived from Eq. [5a] or [5b]:

$$b_{o,i} = \exp(\Delta_a H_i/R \cdot T^{\circ}_{1/2,i}) \qquad [6a]$$

or

$$b_{o,i} = \exp(\Delta_a H_i/R \cdot T^{\circ}_{1/2,i} - (\Delta_a C_{p,i}/R) \cdot \ln T^{\circ}_{1/2,i}). \qquad [6b]$$

Further theoretical considerations on $T^{\circ}_{1/2,i}$ are reported in Ref. (19).

The use of $T^{\circ}_{1/2,i}$ permitted us to achieve the minimum of the function Φ in less time and with more stability of the results than directly employing $b_{o,i}$.

Concerning the computation of $Q_{jk,\text{calc}}$, it could be calculated as the integral heat corresponding to the experimental pressure p_{jk}. However, at this pressure the values of $n_{jk,\text{calc}}$ could differ, even considerably, from $n_{jk,\text{expl}}$, in particular when optimization was in progress. In this way, the error on the isotherm would have been added to the error on the integral heat. The first kind of error was already taken into account in the first summation of Eq. [4], and it would have been twice considered. As a consequence, we preferred to compare in Eq. [4] $Q_{jk,\text{expl}}$ to a $Q_{jk,\text{calc}}$ evaluated at a value of coverage equal to $n_{jk,\text{expl}}$. For the evaluation of $Q_{jk,\text{calc}}$, the computing program employed a fictive pressure, p^*, at which a total surface coverage corresponding to $n_{jk,\text{expl}}$ could be calculated by employing the adsorption parameters and the site distribution of a given step of the calculation. The effective pressure, p_{jk}, could differ even considerably from p^* during the intermediate steps of computation. However, at the end of the calculation, the difference between p_{jk} and p^* was generally acceptable. The absolute value of the differences between p_{jk} and p^* (in Torr) averaged 0.09 for Al_2O_3, 0.12 for BeO, 0.06 for Nb_2O_5, 0.10 for TiO_2, 0.08 for WO_3, and 0.10 for ZrO_2. The use of the procedure involving the fictive pressure p^* in the computations ensured that the errors on isotherms and on integral heats were taken in an independent way. The logic of the procedure can be easily understood by an inspection of the flow sheet of the program reported in Fig. 1.

The optimization program was designed to consider up to nine types of different adsorption sites. It had also the possibility of taking into account the dependence of $\Delta_a H_i$ on temperature by taking into account the heat capacity of adsorption as a further parameter.

RESULTS AND DISCUSSION

The experimental results are presented in Figs. 2–4 respectively as isotherms, and as integral and incremental (differential) heats of NH_3 adsorption, measured at 80 and 150°C, for each studied oxide.

Each point of the isotherm at 80°C lies above the corresponding one at 150°C at the same pressure (Fig. 2). This is in agreement with thermodynamics, as ammonia chemisorption is less favored at higher temperature, being an exothermic reaction. Directly from the isotherms of Fig. 2, it is possible to make rough comparisons among the oxides in terms of the number of acid sites titrated. The

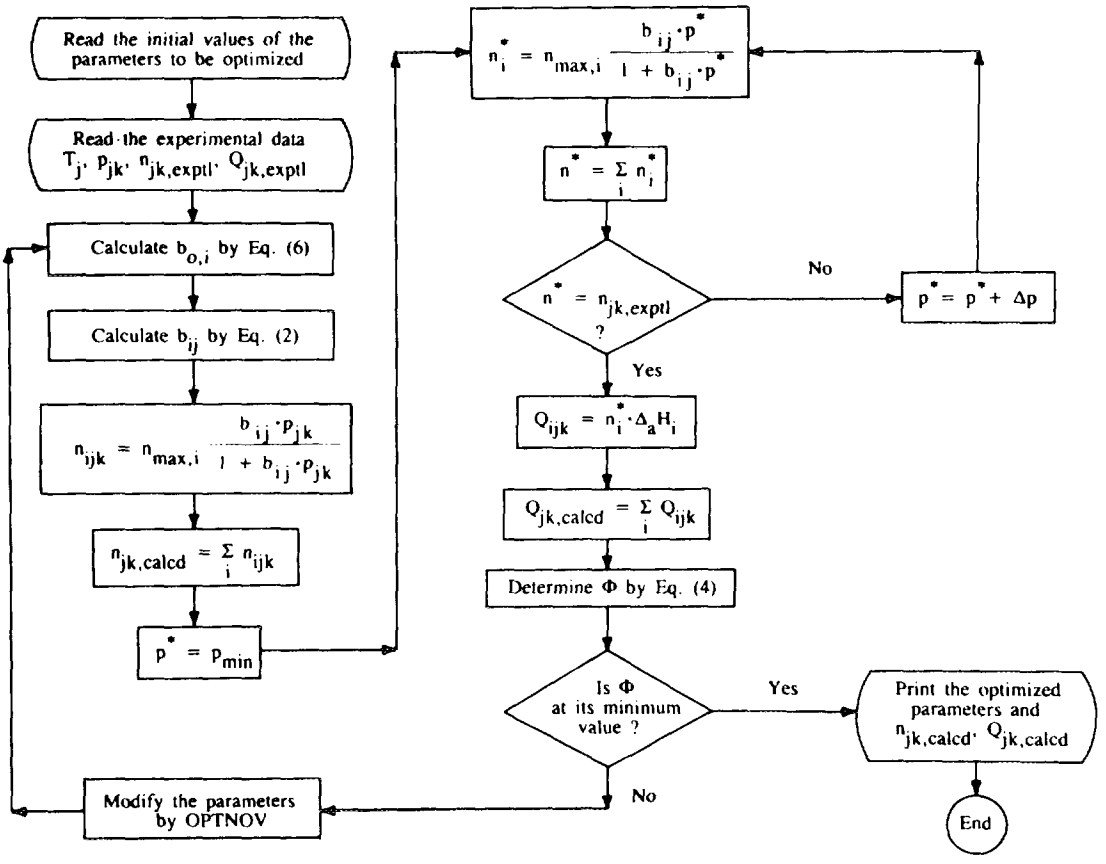

FIG. 1. Flow sheet of the optimization program.

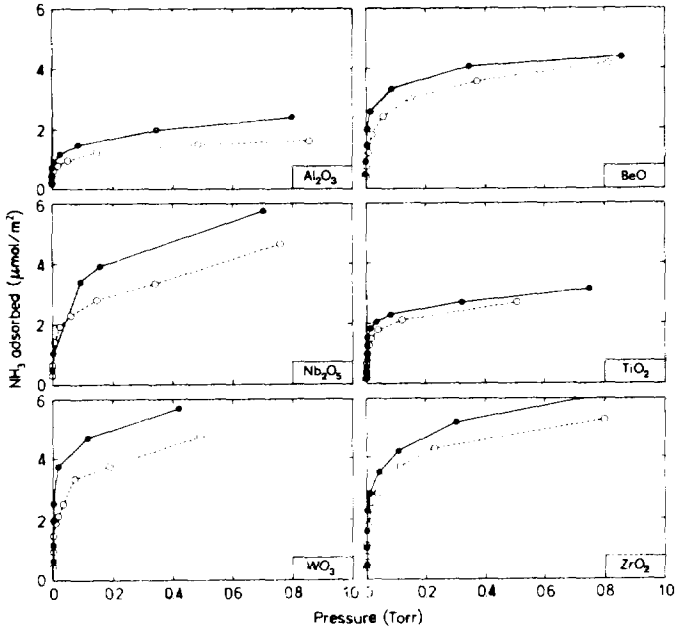

FIG. 2. Adsorption isotherms of ammonia for the different oxides at 80°C, filled symbols, and 150°C, open symbols.

comparisons have to be performed at given pressures. For instance, the following scale of acidity can be found at 0.5 Torr:

$$WO_3 > ZrO_2 > Nb_2O_5 > BeO > TiO_2 > Al_2O_3.$$

The order of the scale does not change when considering the two different adsorption temperatures.

The integral heat curves (Q vs n) at 80°C lie above those at 150°C for coverage of ammonia higher than 1.5–2 μmol/m² (Fig. 3). For lower coverage, only slight differences between the curves at the two temperatures were observed. A greater integral heat at lower temperature for a given coverage is also justified by thermodynamics. In fact, as ammonia chemisorption is an exothermic process, the stronger the sites (i.e., the higher the absolute value of $\Delta_a H_i$), the greater the lowering of the adsorption constant with temperature. As a consequence, at lower temperature a larger fraction of the strongest sites is covered, provided kinetics allows equilibrium to be achieved, as pointed out above.

As a general trend, the curves describing the differential heat of adsorption vs the amount of adsorbed NH_3 present a fast and almost monotonic decrease (Fig. 4). However,

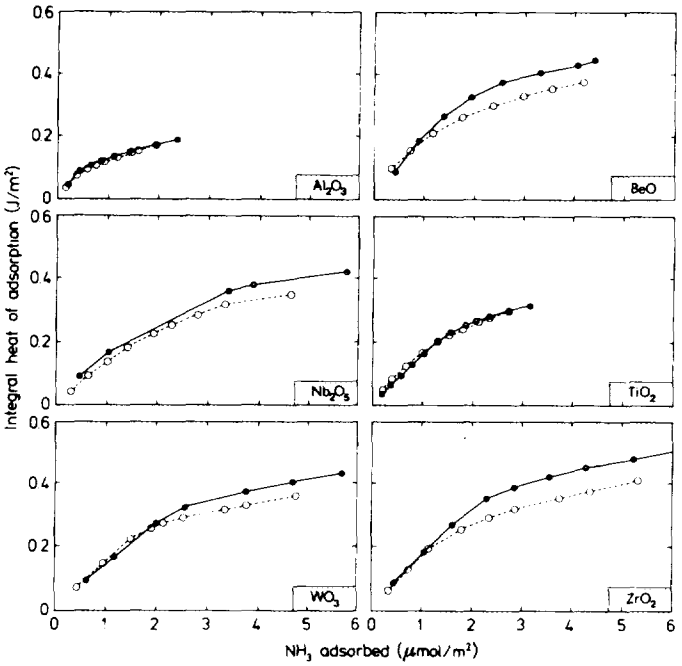

FIG. 3. Integral heat of adsorption of ammonia as a function of coverage for the different oxides at 80°C, filled symbols, and 150°C, open symbols.

an inspection of Fig. 4 shows that differences were observed when curves obtained at the two temperatures were compared. In particular, BeO, ZrO_2, and WO_3 showed more remarkable differences than the other oxides. For each oxide, the strength distribution of the acid sites which one can obtain from the two single curves would be different. Obviously, neither of these observed distributions corresponds to the "true" one.

To obtain the "true" acid site distribution in terms of energy of adsorption, we followed an approach that took into account at the same time the volumetric and calorimetric data collected at the two temperatures. The data were interpreted following the mathematical model described above. The characteristic parameters of the single types of site were optimized through a fitting procedure of the isotherms as well as of the integral heat curves.

The adsorption of ammonia on all the oxides was assumed to be a nondissociative chemisorption with 1 : 1 stoichiometry. As stated above, the total number of ith type sites was a fraction of the overall monolayer coverage of the oxide surface, whose value of 12 μmol/m^2 was calculated on the basis of the cross-sectional area of the adsorbate molecule (20).

During the optimization treatment, the values of adsorption enthalpies were searched in the range from -360 to -40 kJ/mol. The range was chosen on the basis of the experimental values of the differential heat of adsorption, q (Fig. 4). Actually, the q values did not exceed 300 kJ/mol. However, the highest q values could contain the contribution of stronger sites, as they were average values relevant to heterogeneous surfaces ($q = -\Delta_a\overline{H}$). For this reason, the range of the enthalpies of adsorption was extended up to -360 kJ/mol. On the other hand, the range -360 to -40 kJ/mol is the typical enthalpy-of-adsorption range of chemisorption.

In the computations, the whole range of enthalpy was generally divided in equally spaced bands, optimizing the other parameters, namely the various $n_{\max,i}$ and either $b_{o,i}$ or $T^{\circ}_{1/2,i}$. No more than nine different values of enthalpies, which means nine different types of site, were considered at the same time. Such a number of possible different types of site seemed large enough. In fact, no more than four types of site were ever found for all oxides in preliminary computations carried out without dividing the enthalpy range in fixed bands.

In most optimizations, the values of $\Delta_a H_i$ were kept independent of temperature. When the temperature dependence of $\Delta_a H_i$ was considered by introducing the heat capacity of adsorption as a further parameter to be optimized, only a small influence of this last parameter was observed. Actually, the variation of enthalpy of adsorption should be significant only for large temperature differences, otherwise its correction through the use of $\Delta_a C_{p,i}$ should be rather small (of the order of few kJ in the temperature range considered) (7, 8).

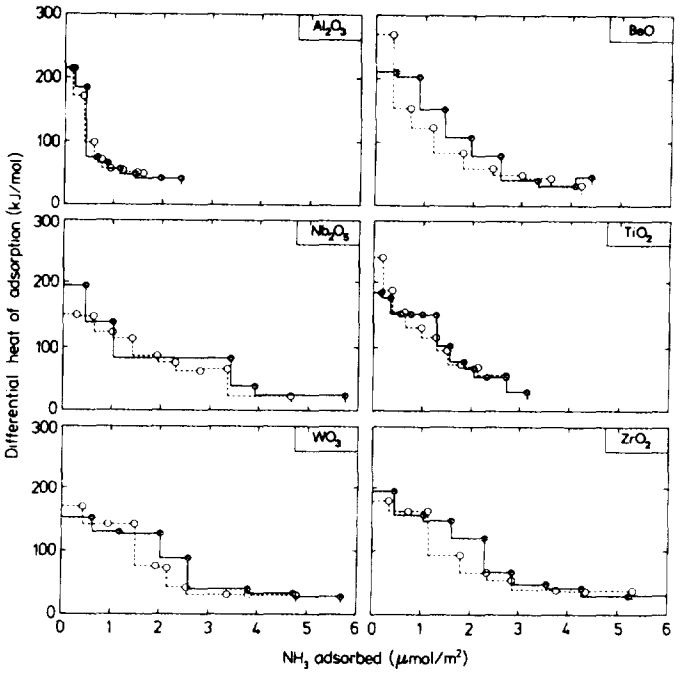

FIG. 4. Differential heat of adsorption of ammonia as a function of coverage for the different oxides at 80°C, filled symbols, and 150°C, open symbols.

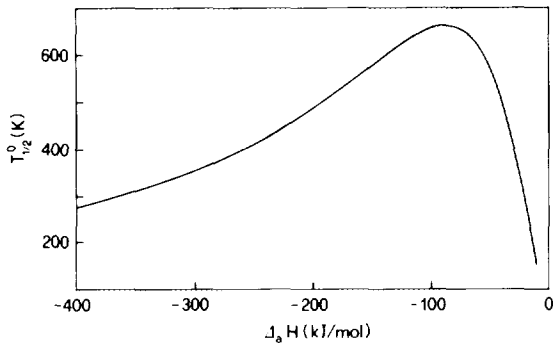

FIG. 5. Dependence of $T^{\circ}_{1/2}$ on enthalpy of adsorption for Al_2O_3 following Eq. [7] with A and B parameters of Table 1.

In preliminary computations, $b_{o,i}$ parameters were optimized instead of the $T^{\circ}_{1/2,i}$ which were used subsequently. A clear dependence of $b_{o,i}$ on $\Delta_a H_i$ was noticed, even though it was difficult to be quantitatively expressed. Such a dependence is an example of the so-called "compensation effect" (21). It was expected, as the rotation and vibration of an adsorbed molecule ought to be affected by the value of the adsorption energy (15).

Due to the relation between $b_{o,i}$ and $T^{\circ}_{1/2,i}$ (Eqs. [6a] and [6b]), a relation of $T^{\circ}_{1/2,i}$ with $\Delta_a H_i$ should exist, too. Also it would be expected that $T^{\circ}_{1/2,i}$ should be different for sites having different strength. The dependence of $T^{\circ}_{1/2,i}$ on $\Delta_a H_i$ was studied by means of optimizations of $n_{max,i}$ and $T^{\circ}_{1/2,i}$ parameters carried out considering four types of site for each oxide. Two different enthalpy ranges were employed: the range -360 to -40 kJ/mol in a first series of computations and the range -320 to -80 kJ/mol in a second series. Analogous results were obtained in both cases. A relation between the two parameters, corresponding to the following equation, was obtained

$$1/T^{\circ}_{1/2,i} = A/\Delta_a H_i + B \cdot \Delta_a H_i, \qquad [7]$$

where A and B are two constant coefficients. In fact, a linear relation was observed for all the oxides plotting $\Delta_a H_i/T^{\circ}_{1/2,i}$ vs $\Delta_a H_i^2$.

Following Eq. [7], $T^{\circ}_{1/2,i}$ increases with $\Delta_a H_i$ for high $|\Delta_a H_i|$ values, while an opposite trend holds for low values of $|\Delta_a H_i|$ (Fig. 5). The increasing trend of $T^{\circ}_{1/2,i}$ vs $\Delta_a H_i$, corresponding to a lowering of $T^{\circ}_{1/2,i}$ with the site strength, was expected. In fact, the more exothermic the sites are, the lower should be the temperature at which the same coverage is reached at a given pressure. However, such a trend cannot hold down to very low $|\Delta_a H_i|$ values as the adsorption process tends to vanish when $|\Delta_a H_i| \to 0$. Thus, the inversion of the trend for low $|\Delta_a H_i|$ values, supported by Eq. [7], is justified.

The final computations were carried out by optimizing the $n_{max,i}$ parameters and the A and B coefficients of Eq. [7] for each oxide keeping a discrete fixed division of $\Delta_a H_i$ range, namely nine values between -360 and -40 kJ/mol with band of 40 kJ/mol. The final parameters are collected in Table 1 together with the $T^{\circ}_{1/2,i}$ values calculated on the basis of Eq. [7].

Some chosen examples of comparison between experimental and calculated isotherms as well as integral heat curves are shown in Figs. 6 and 7. The calculated curves were obtained by means of the optimum parameters of Table 1. In the figures, the curves relevant to the single types of site are also reported.

The goodness of fit can be evaluated on the basis of the standard errors of the estimate of the total number of adsorbed moles and of the integral heats reported as percentages in Table 1. Except for TiO_2, for which the error was as high as 36%, the standard errors averaged around 20% for all the oxides. Such errors can be acceptable, although they are relatively large. The goodness-of-fit was different for the volumetric and the calorimetric data, and for the different temperatures. In most cases, the isotherms could be fitted better than the integral heat curves, and the data at 80°C better than those at 150°C. The more difficult fitting of the calorimetric data can be justified, since the procedure followed for computing the optimum calorimetric curves was less direct compared with the method used for the isotherms. The largest errors shown by TiO_2 are due to the poor fit of the data at 150°C. Probably the adsorption of ammonia on TiO_2 is a more complex phenomenon than the one described by the model employed.

Table 1 shows that the values of $T^{\circ}_{1/2,i}$ appear to be roughly the same at a given $\Delta_a H_i$ for all the oxides. Moreover, the value of $T^{\circ}_{1/2,i}$ for the strong acid sites ($\Delta_a H_i = -280$, -200, and -160 kJ/mol) decreases when the strength of the sites increases. The value of $T^{\circ}_{1/2,i}$ attains a plateau or slightly decreases going towards weaker sites, for which the adsorption is less exothermic. The overall trend of $T^{\circ}_{1/2,i}$, which follows the empirical Eq. [7], has been rationalized above. The various optimized A and B coefficients of this equation are reported in Table 1.

On the basis of the total number of acid sites (n_{max}) found for the different oxides and collected in Table 1, the scale of acidity derived above from the preliminary examination of the experimental data can be confirmed.

Concerning the site energy distribution, no more than three or four different types of site were found for each oxide, even though the computation took into account up to nine types. It is known that ammonia can adsorb on metal oxide surfaces in only a few modes; four principal modes have been reported (22, 23). All the oxides showed a significant quantity of sites (70–80% of the total) associated with a $\Delta_a H_i$ of -40 kJ/mol. These sites are probably related to hydrogen-bonded ammonia, the weakest mode

TABLE 1

Optimized Adsorption Parameters and Standard Errors of the Estimates

Oxide	$\Delta_a H_i$ (kJ mol^{-1})	$n_{max,i}$ (μmol m^{-2})	T° (mol · kJ^{-1} · K^{-1})	n_{max}[b] (μmol m^{-2})	$10^2 \cdot A$[c] (kJ · mol^{-1} · K^{-1})	$10^6 \cdot B$[c] (mol · kJ^{-1} · K^{-1})	σ_n[d] (%)	σ_Q[e] (%)
Al_2O_3	−280	0.169	375	1.982	−6.52	−8.69	19.4	22.3
	−200	0.211	484					
	−160	0.096	556					
	−40	1.506	506					
BeO	−280	0.672	375	4.557	−6.10	−8.75	19.5	24.4
	−200	0.583	487					
	−40	3.303	534					
Nb_2O_5	−280	0.475	371	4.760	−6.14	−8.83	22.9	24.6
	−200	0.448	482					
	−160	0.154	557					
	−40	3.682	529					
TiO_2	−280	0.693	373	3.197	−6.19	−8.78	36.7	36.3
	−200	0.130	484					
	−160	0.111	558					
	−40	2.262	527					
WO_3	−280	0.533	373	5.553	−5.68	−8.84	15.5	22.6
	−200	0.651	487					
	−40	4.368	563					
ZrO_2	−280	0.709	374	5.496	−6.20	−8.75	26.1	23.5
	−200	0.408	486					
	−160	0.255	560					
	−40	4.124	527					

[a] Calculated by Eq. [7].
[b] $n_{max} = \Sigma\, n_{max,i}$.
[c] Coefficients of Eq. [7].
[d] Standard error of the estimate of the adsorbed molecules.
[e] Standard error of the estimate of the integral heat.

of interaction (22, 23). The other 20–30% of sites were distributed in the $\Delta_a H_i$ range of −160 to −280 kJ/mol, corresponding to more energetic interactions of ammonia with the surface. The acid site energy distribution for all the oxides is depicted comparatively in Fig. 8.

By employing the optimized values of $\Delta_a H_i$ and $T^\circ_{1/2,i}$, the adsorption constants at the two considered temperatures ($b_{i,80}$ and $b_{i,150}$) as well as the preexponential factor of Eq. [2a] ($b_{\circ,i}$) were calculated for each type of site of each oxide (Table 2). One might expect as a trend that the stronger the site, the higher the value of the adsorption constant. Actually, Table 2 shows that b_i values do not montonically increase with $|\Delta_a H_i|$, but they follow a trend passing through a maximum for all the oxides. The b_i values for the strongest sites are even very much lower than the ones for the weakest sites. The reason for this behavior is that the two considered temperatures are too high to give rise to the expected trend. As a matter of fact, a monotonic increase of b_i vs $|\Delta_a H_i|$ is obtainable at temperatures as low as −40 to −50°C, as shown in Fig. 9 which reports the dependence of b_1 on temperature for γ-Al_2O_3 as an example. Increasing temperature, the value of b_i decreases following the linear relation ln b_i vs $1/T$ derivable from Eq. [2a]. The decrease of the b_i values with temperature is, obviously, larger as $|\Delta_a H_i|$ is higher. Intersections between lines can occur (Fig. 9) leading to modifications of the trend of b_i vs. $\Delta_a H_i$.

The values of $b_{\circ,i}$, calculated by means of Eq. [6a] for each $T^\circ_{1/2,i}$, were used to evaluate the molar standard entropy of adsorption for each type of site ($\Delta_a S_i^\circ$) according to the equation suggested by Kemball (24):

$$\Delta_a S_i^\circ = R \ln (p^\circ \cdot b_{\circ,i}) - RT \frac{\partial \ln b_{\circ,i}}{\partial T}. \qquad (8)$$

The pressure p° equal to 1 bar for the gas phase and the half-coverage for the adsorbed phase were adopted as standard states. The term $RT \cdot (\partial \ln b_{\circ,i}/\partial T)$ was consid-

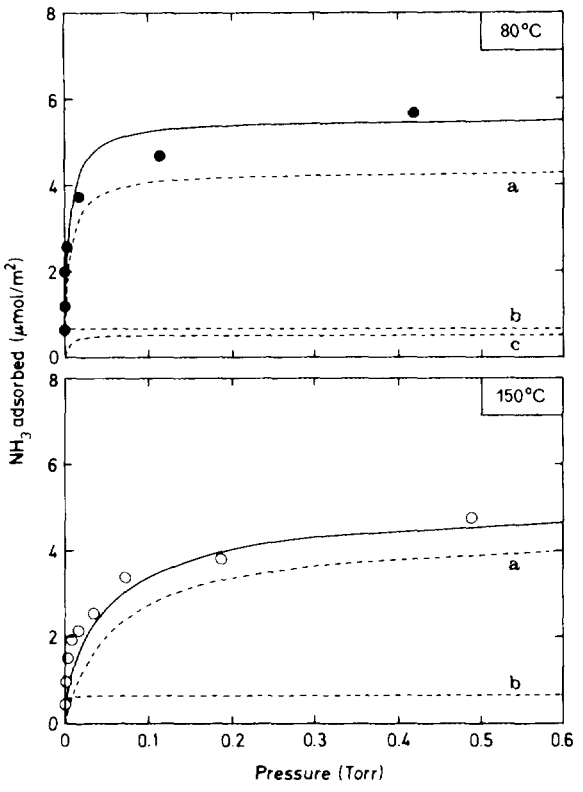

FIG. 6. Adsorption isotherms of ammonia for WO_3 at 80 and 150°C. Symbols, experimental values; solid lines, overall calculated isotherms; dashed lines, calculated isotherms for each type of site of different $\Delta_a H_i$ ((a) −40, (b) −200, (c) −280 kJ/mol). The curves are calculated by the optimized parameters.

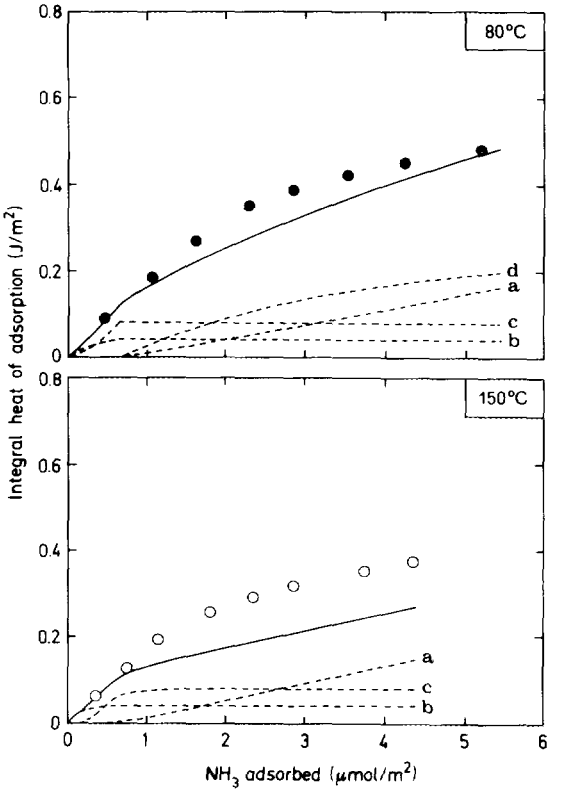

FIG. 7. Integral heats of adsorption of ammonia as a function of coverage for ZrO_2 at 80 and 150°C. Symbols, experimental values; solid lines, overall calculated heats; dashed lines, calculated heats for each type of site of different $\Delta_a H_i$ ((a) −40, (b) −160, (c) −200, (d) −280 kJ/mol). The curves are calculated by the optimized parameters.

ered as ranging between $-R$ and $3R/2$ (24). The entropies calculated for these extreme cases were averaged.

Taking into account the different coverage of the sites of each type and the different $\Delta_a S_i^\circ$ values, it was possible to evaluate the mean molar standard entropy of adsorption ($\Delta_a S^\circ_{calc}$) corresponding to each point of the experimental isotherms:

$$\Delta_a S^\circ_{calc} = \frac{\sum_i n_i \cdot \Delta_a S_i^\circ}{\sum_i n_i}. \qquad [9]$$

As an example, the curves which describe the increase of $\Delta_a S^\circ_{calc}$ with ammonia coverage for BeO at the two considered temperatures are reported in Fig. 10.

The experimental volumetric–calorimetric data can be used directly to evaluate the mean molar standard entropy of adsorption ($\Delta_a S^\circ_{expl}$) by Eq. [10]. This equation derives from that of Garrone *et al.* (25) and was used for the calculation of the entropy of adsorption in the interactions of acidic and basic adsorbates with alumina (26).

$$\Delta_a S^\circ_{expl} = \frac{Q}{T \cdot n} + \frac{R}{n}\int_0^p n\, d\ln p - R\ln(p/p^\circ). \qquad [10]$$

The values obtained in the case of BeO are reported in Fig. 10 for comparison with the $\Delta_a S^\circ_{calc}$ values.

To make a simple comparison between the $\Delta_a S^\circ_{calc}$ and the $\Delta_a S^\circ_{expl}$ for all the investigated oxides, the averaged values of the entropies calculated at the two temperatures

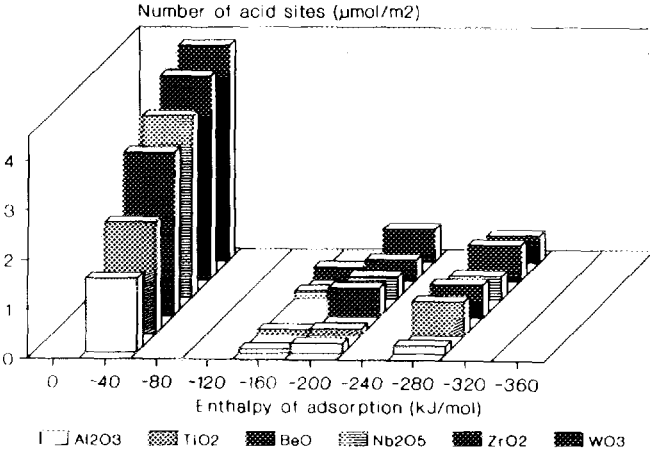

FIG. 8. Acid site energy distribution for all the oxides.

TABLE 2

Thermodynamic Parameters of Adsorption

Oxide	$\Delta_a H_i$ (kJ mol^{-1})	$b_{i,80}$ (Torr^{-1})	$b_{i,150}$ (Torr^{-1})	$b_{o,i}$ (Torr^{-1})	$\Delta_a S^\circ_{calc}$[a] (J · K^{-1} · mol^{-1})	$\Delta_a S^\circ_{expl}$[b] (J · K^{-1} · mol^{-1})
Al_2O_3	−280	$2.56 \cdot 10^2$	$3.61 \cdot 10^{-5}$	$9.87 \cdot 10^{-40}$	−160	−81
	−200	$1.03 \cdot 10^8$	$1.31 \cdot 10^3$	$2.70 \cdot 10^{-22}$		
	−160	$4.31 \cdot 10^8$	$5.25 \cdot 10^4$	$9.33 \cdot 10^{-16}$		
	−40	$6.08 \cdot 10^1$	6.39	$7.38 \cdot 10^{-5}$		
BeO	−280	$2.60 \cdot 10^2$	$3.67 \cdot 10^{-5}$	$1.00 \cdot 10^{-39}$	−172	−129
	−200	$1.33 \cdot 10^8$	$1.70 \cdot 10^3$	$3.49 \cdot 10^{-22}$		
	−40	$1.00 \cdot 10^2$	$1.05 \cdot 10^1$	$1.22 \cdot 10^{-4}$		
Nb_2O_5	−280	$1.10 \cdot 10^2$	$1.55 \cdot 10^{-5}$	$4.25 \cdot 10^{-40}$	−147	−161
	−200	$8.35 \cdot 10^7$	$1.07 \cdot 10^3$	$2.19 \cdot 10^{-22}$		
	−160	$4.45 \cdot 10^8$	$5.41 \cdot 10^4$	$9.63 \cdot 10^{-16}$		
	−40	$9.34 \cdot 10^1$	9.81	$1.13 \cdot 10^{-4}$		
TiO_2	−280	$1.68 \cdot 10^2$	$2.37 \cdot 10^{-5}$	$6.50 \cdot 10^{-40}$	−151	−165
	−200	$1.01 \cdot 10^8$	$1.29 \cdot 10^3$	$2.64 \cdot 10^{-22}$		
	−160	$4.90 \cdot 10^8$	$5.96 \cdot 10^4$	$1.06 \cdot 10^{-15}$		
	−40	$8.87 \cdot 10^1$	9.32	$1.08 \cdot 10^{-4}$		
WO_3	−280	$1.80 \cdot 10^2$	$2.53 \cdot 10^{-5}$	$6.93 \cdot 10^{-40}$	−134	−77
	−200	$1.40 \cdot 10^8$	$1.80 \cdot 10^3$	$3.69 \cdot 10^{-22}$		
	−40	$1.61 \cdot 10^2$	$1.70 \cdot 10^1$	$1.96 \cdot 10^{-4}$		
ZrO_2	−280	$2.28 \cdot 10^2$	$3.21 \cdot 10^{-5}$	$8.80 \cdot 10^{-40}$	−148	−95
	−200	$1.17 \cdot 10^8$	$1.50 \cdot 10^3$	$3.08 \cdot 10^{-22}$		
	−160	$5.40 \cdot 10^8$	$6.57 \cdot 10^4$	$1.17 \cdot 10^{-15}$		
	−40	$8.88 \cdot 10^1$	9.33	$1.08 \cdot 10^{-4}$		

[a] Calculated from $b_{o,i}$ values on the basis of Eq. [9], see text.
[b] Obtained from the volumetric-calorimetric experimental data on the basis of Eq. [10], see text.

for a $n_{max}/2$ coverage ($\Delta_a \bar{S}^\circ_{calc}$ and $\Delta_a \bar{S}^\circ_{expl}$) are collected in Table 2. Even though significant differences can be noticed in some cases, there is evidence that the range of $\Delta_a \bar{S}^\circ_{calc}$ (−130 to −170 J · K^{-1} · mol^{-1}) is included in the relatively narrow range of $\Delta_a \bar{S}^\circ_{expl}$ (−80 to −170 J · K^{-1} · mol^{-1}), typical of immobile or localized adsorption (24).

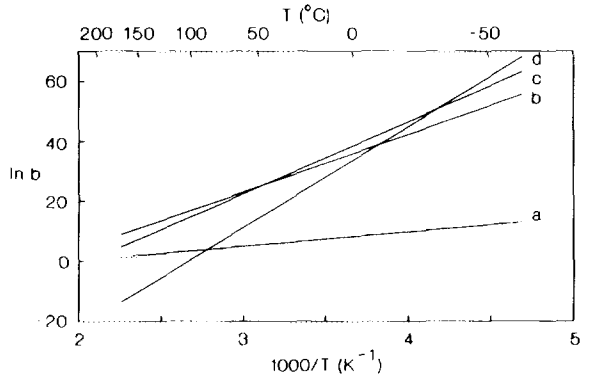

FIG. 9. Dependence of adsorption constants on temperature for NH_3 adsorption on sites of γ-Al_2O_3 of different $\Delta_a H_i$ ((a) −40, (b) −160, (c) −200, (d) −280 kJ/mol).

The adsorption entropies calculated as $\Delta_a S^\circ_{calc}$ were obtained from the $b_{o,i}$ parameters derived from the optimized $T^\circ_{1/2,i}$. They are similar, at least in terms of order of magnitude, to the $\Delta_a S^\circ_{expl}$ values evaluated in a completely different way. This seems a quite good index of the validity of the optimized $T^\circ_{1/2,i}$ parameters.

CONCLUSIONS

The use of two series of data collected by two coupled experimental adsorption techniques (volumetric and calorimetric) at different temperatures, permits one to determine the energy distribution of the acid sites of heterogeneous oxide surfaces.

A maximum of four types of ammonia chemisorption sites was found, in agreement with what is known about the number of the principal modes of ammonia adsorption on metal oxides.

The physicochemical behavior of the adsorbate–adsor-

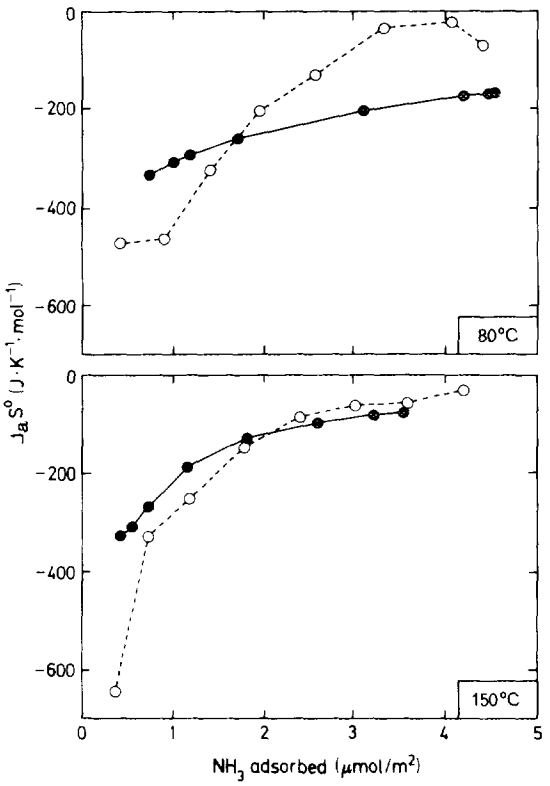

FIG. 10. Standard mean molar entropy of adsorption of ammonia as a function of coverage for BeO at 80 and 150°C. Filled symbols, entropies calculated from $b_{o,i}$ values; open symbols, entropies evaluated from the volumetric–calorimetric experimental data (see test).

bent system was adequately represented by the proposed model. This allowed us to obtain the thermodynamic adsorption parameters of each type of site, together with their temperature dependence.

The introduction into the computations of the new parameter $T^{\circ}_{1/2,i}$, instead of the usual $b_{o,i}$ preexponential factor, permitted us to reach the minimum of the objective function faster with a higher stability of the final optimized parameters.

REFERENCES

1. Kijenski, J., and Baiker, A., *Catal. Today* **5,** 1 (1989).
2. Tanabe, K., Misono, M., Ono, Y., and Hattori, H., "New Solid Acids and Basis, Their Catalytic Properties," Stud. Surf. Sci. Catal. Series, Vol. 51, Chap. 2. Elsevier, Amsterdam, 1989.
3. Lemaitre, J. L., *in* "Characterization of Heterogeneous Catalysts" (F. Delannay, Ed.), p. 29. Dekker, New York, 1984.
4. Hashimoto, K., Masuda, T., and Mori, T., *in* "New Developments in Zeolite Science and Technology" (Y. Murakami, A. Iijima, and J. M. Ward, Eds.), p. 503. Kodansha/Elsevier, Tokyo/Amsterdam, 1986.
5. Auroux, A., *in* "Les Techniques Physiques d'Etude des Catalyseurs" (B. Imelik, and J. C. Védrine, Eds.), p. 823. Technip, Paris, 1988.
6. Fubini, B., *Thermochim. Acta* **135,** 19 (1988).
7. Cardona-Martinez, N., and Dumesic, J. A., *Adv. Catal.* **38,** 149 (1992).
8. Tsutsumi, K., Mitani, Y., and Takahashi, H., *Bull. Chem. Soc. Jpn.* **56,** 1912 (1983).
9. Cardona-Martinez, N., and Dumesic, J. A., *J. Catal.* **125,** 427 (1990).
10. Auroux, A., and Gervasini, A., *J. Phys. Chem.* **94,** 6371 (1990).
11. Gervasini, A., and Auroux, A., *J. Catal.* **131,** 190 (1991).
12. Gervasini, A., and Auroux, A., *J. Thermal Anal.* **37,** 1737 (1991).
13. Langmuir, I., *J. Am. Chem. Soc.* **40,** 1361 (1918).
14. Klyachko, A. L., *Kinet. Katal.* **19,** 1218 (1978).
15. Jaroniec, M., and Madey, R., "Physical Adsorption on Heterogeneous Solids", Chap. 2. Elsevier, Amsterdam, 1988.
16. Rudzinski, W., and Everett, D. H., "Adsorption of Gases on Heterogeneous Surfaces", Chap. 5. Academic Press, London, 1992.
17. Buzzi Ferraris, G., *Ing. Chim. Ital.* **4,** 171, 180 (1968).
18. Koubek, J., Pašek, J. and Volf, J., *J. Colloid Interface Sci.* **51,** 491 (1975).
19. Carniti, P., and Gervasini, A., *React. Kinet. Catal. Lett.*, in press.
20. Emmett, P. H., and Brunauer, S., *J. Am. Chem. Soc.* **59,** 1553 (1937).
21. Galwey, A. K., *Adv. Catal.* **26,** 247 (1977) and references therein.
22. Tsyganenko, A. A., Pozdnyakov, D. V., Filimonov, V. N., *J. Mol. Struct.* **29,** 299 (1975).
23. Labus, S., *Zesz. Nauk. Gorn.-Hutn. im. Stanislawa Staszica Chem.* **665,** 91 (1978).
24. Kemball, C., *Adv. Catal.* **2,** 233 (1950).
25. Garrone, E., Rouquérol, F., Fubini, B., and Della Gatta, G., *J. Chim. Phys.* **76,** 528 (1979).
26. Gervasini, A., and Auroux, A., *J. Phys. Chem.* **97,** 2628 (1993).